

Small size instanton contributions to the quark quasi-PDF and matching kernel

Yizhuang Liu*

*Tsung-Dao Lee Institute, Shanghai Jiao Tong University, Shanghai, 200240, China
Institut für Theoretische Physik, Universität Regensburg, D-93040 Regensburg, Germany*

Ismail Zahed†

*Center for Nuclear Theory, Department of Physics and Astronomy,
Stony Brook University, Stony Brook, New York 11794-3800, USA*

We investigate the non-perturbative contribution of instantons to current matching kernels used in the context of the large momentum effective theory (LaMET). We derive explicitly these contributions using first principle semi-classical calculus for the unpolarized and polarized quark parton distributions and the matching kernel, and show that they are part of a trans-series expansion. These contributions are substantial at current lattice matching momenta.

I. INTRODUCTION

Light cone distributions are central to the description of hard inclusive and exclusive processes. Thanks to factorization, a hard process factors into a perturbatively calculable contribution times pertinent parton distribution and fragmentation functions. Standard examples can be found in deep inelastic scattering, Drell-Yan process and jet production to cite a few. The parton distribution functions are defined on the light front, and their moments usually fitted using large empirical data bank. They are not readily amenable to a non-perturbative and first principle formulation using lattice simulations.

Ji [1] has put forth the concept of quasi-parton distributions as a way to approach the light cone parton distributions from first principles on the lattice [2–7]. The idea is to start from pertinent partonic correlators at equal-time in a boosted hadron state, which are amenable to an Euclidean formulation. Under increasing boosts, these quasi-distributions asymptote the light cone distributions space-like. They are conjectured to map onto their time-like analogue through perturbative matching. This conjecture can be checked to hold non-perturbatively in two-dimensional QCD and at sub-leading order in the large number of color limit [8]. Some variants of this formulation can be found in the form of pseudo distributions [9], and lattice cross sections [10].

A number of QCD lattice collaborations have implemented some of these ideas with some reasonable success in extracting the light cone parton distributions through matching.

* yizhuang.liu@sjtu.edu.cn

† ismail.zahed@stonybrook.edu

Unfortunately, most simulations become increasingly noisy as the boosting is increased, making the extraction by matching limited to boosting momenta of the order of few GeV. In this range, the power corrections and non-perturbative effects are still sizable even in the matching kernel. The chief motivation of this analysis is to estimate some of these non-perturbative contributions from first principles, using QCD semi-classics.

Several QCD lattice simulations have shown that the bulk characteristics and correlations in the QCD vacuum are mostly unaffected by lattice cooling [11] where quantum effects are pruned, suggesting that semi-classical gauge and fermionic fields dominate the ground state structure. At weak coupling, instantons and anti-instantons are exact classical gauge tunneling configurations with large actions and finite topological charge which support exact quark zero modes with specific chirality.

The large size instanton and anti-instanton configurations in the QCD vacuum are at the origin of the spontaneous breaking of chiral symmetry and the origin of mass. They still lack the long-range characteristics of the gauge fields necessary for the disordering of the large Wilson loops in the quenched approximation, although some form of screening in the full theory may not require that.

The small size instantons and anti-instantons configurations contribute ideally to short distance processes through weak coupling semi-classics, although they become increasingly rare as their density wanes out. It is the purpose of this work to explore their contribution to matching kernels in the quasi-parton approach [12], following the recently suggested program to consider the role of small size instantons in semi-inclusive processes [13]. Our analysis readily extends to the pseudo-parton program and lattice cross sections.

The outline of the paper is as follows: in section II we briefly review some bulk aspects of the large and small instantons that are relevant for this work, with a particular discussion on the size averaging procedure. In section III we provide results for two complementary LSZ reductions in Euclidean space. In section IV we derive the contribution of a random ensemble of instantons and anti-instantons to the unpolarized quark parton distributions. In section IV D the results are extended to the polarized distributions where the mixing between zero modes and non-zero modes is dominant. In section V a one-loop gluon effect in the instanton background is considered and shown to yield a large correction to the perturbative matching kernel. Our conclusions are in section VI.

II. INSTANTON EFFECTS

The bulk characteristics of the instanton liquid model are captured by the parameters [14]

$$n_{I+\bar{I}} \approx 1/L^4 \approx 1/\text{fm}^4 \quad \rho \approx (1/3) \text{ fm} \approx 1/(0.6 \text{ GeV}) \quad (1)$$

for the instanton plus anti-instanton density and size, respectively. They combine in the dimensionless packing parameter $\kappa \equiv \pi^2 \rho^4 n_{I+\bar{I}} \approx 0.1$, a measure of the diluteness of the instanton-anti-instanton ensemble in the QCD vacuum. Previous lattice simulations using cooling methods support these observations, see [15] for a review.

A more recent lattice simulation aimed at extracting the running gauge coupling constant with momentum [16], through a pertinent ratio of 2- and 3-point gluonic functions, has suggested a larger instanton density with $\kappa \approx 1$. This observation at large running momenta, points at the effects from the smaller size instanton-anti-instanton configurations which are likely to affect short distance physics such as the running of the coupling, with negligible effects on the longer range mechanism of chiral symmetry breaking.

Small size instanton fields are strong, since their field strength is large. In fact, even for dominant and large size instantons with $\rho \approx 0.30$ fm typical for chiral symmetry breaking, it is still sizable, with typical chromo-electric and -magnetic fields $E = B \approx \sqrt{48}/\rho^2 \approx 2.5$ GeV². These fields are comparable to the current momentum extrapolations using LaMET in the hard matching kernel. Their short distance contribution can be assessed using semi-classics. For many estimates it is sufficient to use the fixed value of $\rho \approx 0.30$ fm. However, in harder kernels the small size instantons are dominant, but their density is suppressed [17, 18]

$$\frac{dn(\rho)}{d\rho} \approx \frac{1}{\rho^5} (\rho \Lambda_{QCD})^{b_{QCD}} e^{-C\rho^2/L^2} \quad (2)$$

with $b_{QCD} = 11N_c/3 - 2N_f/3 \approx 9$ (one loop) and C a number of order 1. This notwithstanding, in this regime the effective gauge coupling is weak, the action is large and the use of the semi-classical approximation is justified, with the instanton contribution leading and the gluon exchange contribution subleading. We will limit the hard instanton contributions to $\rho \leq \rho_S$ in the hard kernel, and relegate the contributions from larger instantons with $\rho \geq \rho_S$ to the wavefunctions [19].

III. LSZ REDUCTION IN INSTANTON BACKGROUND

We start by recalling briefly the LSZ reduction formula for the instanton. We note that the LSZ reduction is not guaranteed unless the Euclidean field theory has an Hamiltonian interpretation, which is lacking in the instanton model of the QCD vacuum. Here it is understood as an algorithm, following the initial suggestions in [20, 21]. We will present the reduction in two different limits: 1/ the zero Euclidean momentum limit; 2/ the large Euclidean time limit. Both construction yield similar results modulo an infrared sensitivity noted only in the first approach. The first reduction was recently used in the discussion of the instanton contributions to the mesonic form-factors [13].

A. Fermion propagator in an instanton

The full non-zero propagator in the instanton background in the chiral-split form reads [22]

$$\begin{aligned} S_{nz}(x, y) &= \overrightarrow{\mathcal{D}}_x \Delta(x, y) \frac{1 + \gamma_5}{2} + \Delta(x, y) \overleftarrow{\mathcal{D}}_y \frac{1 - \gamma_5}{2} \\ &= \overline{S}(x, y) \frac{1 + \gamma_5}{2} + S(x, y) \frac{1 - \gamma_5}{2} \end{aligned} \quad (3)$$

with the free Weyl propagators $S_0 = 1/\overline{\partial}$ and $\overline{S}_0 = 1/\partial$, in the notations detailed in Appendix A. The long derivative $\overrightarrow{\mathcal{D}} = \overrightarrow{\partial} - i\overrightarrow{\mathcal{A}}$ acts on the left and right respectively of the (massless) scalar propagator,

$$\Delta(x, y) = \Delta_0(x - y) \left(1 + \rho^2 \frac{[Ux\bar{y}U^\dagger]}{x^2 y^2} \right) \frac{1}{(\Pi_x \Pi_y)^{\frac{1}{2}}} \quad (4)$$

with $\Delta_0(x) = 1/(2\pi x)^2$ the free scalar propagator, and $\Pi_x = 1 + \rho^2/x^2$, and x, \bar{y} are convoluted with (Euclidean 4d) sigma matrices (A1). Each explicit contribution is

$$\begin{aligned} \overline{S}(x, y) &= \left(\overline{S}_0(x - y) \left(1 + \rho^2 \frac{[Ux\bar{y}U^\dagger]}{x^2 y^2} \right) + \frac{\rho^2 \overline{\sigma}_\mu [Ux\overline{\sigma}_\mu(x - y)\bar{y}U^\dagger]}{4\pi^2 \Pi_x x^4 (x - y)^2 y^2} \right) \frac{1}{(\Pi_x \Pi_y)^{\frac{1}{2}}} \\ S(x, y) &= \left(S_0(x - y) \left(1 + \rho^2 \frac{[Ux\bar{y}U^\dagger]}{x^2 y^2} \right) + \frac{\rho^2 \sigma_\mu [Ux(\bar{x} - \bar{y})\sigma_\mu \bar{y}U^\dagger]}{4\pi^2 x^2 (x - y)^2 y^4 \Pi_y} \right) \frac{1}{(\Pi_x \Pi_y)^{\frac{1}{2}}} \end{aligned} \quad (5)$$

and with U valued in $SU(N_c)$. When a mixture of color and spinor indices occurs, the spinor matrices act on the upper left corner of the $N_c \times N_c$ color matrices. The zero modes and their LSZ reduction are discussed in Appendix B.

The effects of the quark masses on the quark propagator in the instanton or anti-instanton fields, are not known in closed form. However, for small masses, the propagator can be expanded around the chiral limit, and in the instanton field it reads

$$\frac{\Psi_0(x, \cdot) \Psi_0^\dagger(y)}{im} + S_{nz}(x, y) - im \left(\Delta(x, y) \frac{1 + \gamma_5}{2} + \int d^4 z \overline{S}(x, z) S(z, y) \frac{1 - \gamma_5}{2} \right) + \mathcal{O}(m^2) \quad (6)$$

Note the chiral mixing induced by the mass m . In the expansion of correlators, the $\mathcal{O}(m)$ term may combine with the $\mathcal{O}(1/m)$ term, to yield a finite $\mathcal{O}(m^0)$ contribution. This will be the case below for the unpolarized quark quasi-PDF.

B. Euclidean zero momentum limit

The LSZ reduction of the quark propagator $S(x, y)$ in an instanton background, is obtained by say taking its half Fourier transform $S(k, y)$, reducing it through $\mathcal{S}(k, y)$, expanding the result around the Euclidean point $k^2 \approx 0$ and analytically continuing the result to Minkowski space. In the chiral split form (5), the reduction for $S\bar{k}$ and $k\bar{S}$ give [21]

$$\begin{aligned} ik\bar{S}(k, z_+) &\approx \frac{e^{+ik \cdot z_+}}{\Pi_+^{1/2}} \left(1 + \frac{\rho^2}{2z_+^2} \frac{Uk\bar{z}_+U^\dagger}{k \cdot z_+} (1 - e^{-ik \cdot z_+}) \right) \\ S(z_-, k)i\bar{k} &\approx \frac{e^{-ik \cdot z_-}}{\Pi_-^{1/2}} \left(1 + \frac{\rho^2}{2z_-^2} \frac{Uz_- \bar{k}U^\dagger}{k \cdot z_-} (1 - e^{+ik \cdot z_-}) \right) \end{aligned} \quad (7)$$

with $z_\pm = (\pm z/2, z_\perp)$, while for the more involved reductions $\bar{S}k$ and $\bar{k}S$ one has [13]

$$\begin{aligned} \bar{S}(z_-, k)i\bar{k} &\approx \frac{e^{-ik \cdot z_-}}{\Pi_-^{1/2}} \left(1 - \frac{\rho^2}{2z_-^2} \frac{Uk\bar{z}_-U^\dagger}{k \cdot z_-} \left(1 - \frac{i}{k \cdot z_-} (1 - e^{+ik \cdot z_-}) \right) - \frac{\rho^2}{m^2} \frac{ik}{z_-^4 \Pi_-} \bar{\sigma}_\mu U z_- \bar{\sigma}_\mu U^\dagger \right) \\ i\bar{k}S(k, z_+) &\approx \frac{e^{+ik \cdot z_+}}{\Pi_+^{1/2}} \left(1 - \frac{\rho^2}{2z_+^2} \frac{Uz_- \bar{k}U^\dagger}{k \cdot z_+} \left(1 + \frac{i}{k \cdot z_+} (1 - e^{-ik \cdot z_+}) \right) - \frac{\rho^2}{m^2} \frac{i\bar{k}}{z_+^4 \Pi_+} \sigma_\mu U \sigma_\mu \bar{z}_+ U^\dagger \right) \end{aligned} \quad (8)$$

Note that the Euclidean regulator $-k^2 \approx 0 \rightarrow m^2$ was used in the last contributions appearing in (8). This infrared sensitivity will be circumvented below through an alternative reduction scheme that is more commensurate with QCD lattice formulations.

C. Euclidean large time limit

An alternative reduction scheme that will prove to be infrared safe with an almost identical outcome, consists in taking the large Euclidean time asymptotics instead, to put the quark on mass shell, a common procedure on the lattice. Specifically, the right reduction of \bar{S} is

$$\lim_{T \rightarrow -\infty} \int d^3 \vec{y} e^{-i\vec{p} \cdot \vec{y}} \bar{S}(x; \vec{y}, T) \quad (9)$$

to bring the massless quark on the energy shell without recourse to the Fourier transform and the external leg reduction. With this in mind, and collecting the results (C2-C7) from Appendix C, we obtain the large time LSZ reduced results for the non-zero mode \bar{S} of the quark propagator in an instanton background

$$\int d^3\vec{y} e^{-i\vec{p}\cdot\vec{y}} \bar{S}(x; \vec{y}, T) = \frac{e^{-|T||\vec{p}|} e^{-T_1|\vec{p}| - i\vec{p}\cdot\vec{x}}}{\Pi_x^{\frac{1}{2}}} \times \left(\frac{1}{2} \mathcal{P}_- - \frac{1}{4x^2} \mathcal{P}_- |\vec{p}| \rho^2 U x \mathcal{P}_- U^\dagger I_-^1 - \frac{\rho^2}{4x^4 \Pi_x} \bar{\sigma}_\mu U x \bar{\sigma}^\mu x \mathcal{P}_- U^\dagger I_- - \frac{\rho^2}{2x^4 |\vec{p}| \Pi_x} \bar{\sigma}_\mu U x \bar{\sigma}^\mu U^\dagger \right), \quad (10)$$

with

$$\begin{aligned} I_-^n &= \int_0^1 dt t^n e^{i(1-t)\vec{x}\cdot\vec{p} + (1-t)T_1|\vec{p}|} \\ I_- &= \int_0^1 dt e^{i(1-t)\vec{x}\cdot\vec{p} + (1-t)T_1|\vec{p}|} \end{aligned} \quad (11)$$

Similarly, we have

$$\int d^3\vec{y} \bar{S}(T, \vec{y}; x) e^{i\vec{p}\cdot\vec{y}} = \frac{e^{-|T||\vec{p}|} e^{T_1|\vec{p}| + i\vec{p}\cdot\vec{x}}}{\Pi_x^{\frac{1}{2}}} \times \left(\frac{1}{2} \mathcal{P}_- + \frac{1}{4x^2} \mathcal{P}_- |\vec{p}| \rho^2 U \mathcal{P}_+ \bar{x} U^\dagger I_+^1 + \frac{\rho^2}{8x^2} |\vec{p}| \bar{\sigma}_\mu U \mathcal{P}_+ \bar{\sigma}^\mu \mathcal{P}_+ \bar{x} U^\dagger I_+ \right), \quad (12)$$

with

$$\begin{aligned} I_+^n &= \int_0^1 dt t^n e^{-i(1-t)\vec{x}\cdot\vec{p} - (1-t)T_1|\vec{p}|} \\ I_+ &= \int_0^1 dt (1-t) e^{-i(1-t)\vec{x}\cdot\vec{p} - (1-t)T_1|\vec{p}|} \end{aligned} \quad (13)$$

The helicity projectors are $\mathcal{P}_\pm = 1 \pm \frac{\vec{\sigma}\cdot\vec{p}}{|\vec{p}|}$. The results for the anti-instanton follow by conjugation. Note that the reduction (10) is infrared safe in contrast to (8). We will use it for the analysis to follow.

For completeness, the large time asymptotics for the scalar propagator in the instanton background in the mass expansion (6)

$$\lim_{T \rightarrow -\infty} \int d^3\vec{y} e^{-i\vec{p}\cdot\vec{y}} \Delta(x; \vec{y}, T) \quad (14)$$

follows from the same reasoning with the result

$$\int d^3\vec{y} e^{-i\vec{p}\cdot\vec{y}} \Delta(x; \vec{y}, T) = \frac{e^{-|T||\vec{p}|} e^{-T_1|\vec{p}| - i\vec{p}\cdot\vec{x}}}{\Pi_x^{\frac{1}{2}}} \left(\frac{2\pi^2}{|\vec{p}|} - \frac{\pi^2 \rho^2}{x^2} \mathcal{P}_- U x U^\dagger I_+^0 \right) \quad (15)$$

and similarly for $\Delta(T, \vec{y}; x)$ with the exchange $x \rightarrow \bar{x}$ in the last contribution.

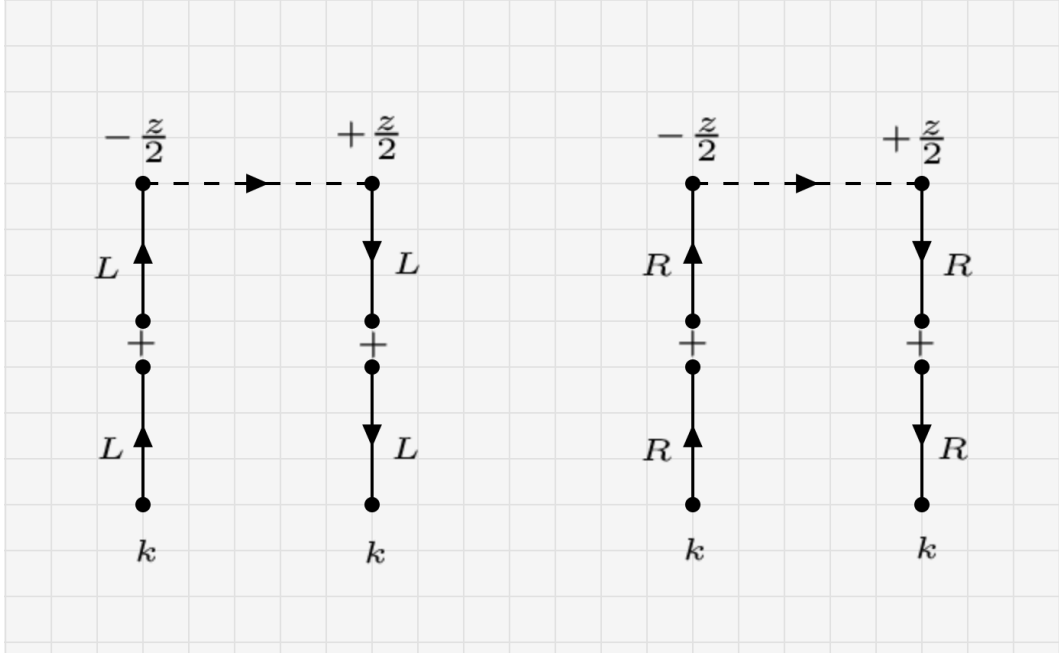


FIG. 1. Non-vanishing small instanton contributions to twist-2 matching factor from only the non-zero modes.

IV. INSTANTON CONTRIBUTION TO THE QUASI-PDF: TREE LEVEL

Given the diluteness of the QCD instanton vacuum with a small packing fraction $\kappa < 1$, it will be sufficient to assess the small size instanton and anti-instanton contributions to the leading twist unpolarized and polarized partonic distributions using the single instanton approximation (SIA) [23, 24]. The approximation is limited to distances which are smaller than the mean distance $L \approx 1$ fm in (1), the distance to the nearest neighbor instanton or anti-instanton in the QCD instanton vacuum. This will be understood throughout. We will carry first this analysis at tree level and correct it to one-loop. The latter correction is important for considerations in relation to the matching kernel in LaMET beyond perturbation theory.

A. Tree Contribution to the unpolarized quark-PDF

The analysis of the quasi-PDF of the light mesons in the context of the random instanton vacuum using the planar approximation, was discussed recently in [19]. Here we study the SIA contribution to the unpolarized quark-PDF. The instanton non-zero mode contributions are illustrated in Fig. 1 and read

$$\begin{aligned} & \frac{n_{I+\bar{I}}}{2} \int d^4 z_I \bar{\chi}_R(P) i \bar{P} S(P, \frac{z}{2} - z_I) \bar{\sigma}^z [+\frac{z}{2}, -\frac{z}{2}]_I S(-\frac{z}{2} - z_I, P) i \bar{P} \chi_R(P) \\ & + \frac{n_{I+\bar{I}}}{2} \int d^4 z_I \bar{\chi}_L(P) i P S(P, \frac{z}{2} - z_I) \sigma^z [+\frac{z}{2}, -\frac{z}{2}]_I S(-\frac{z}{2} - z_I, P) i P \chi_L(P), \end{aligned} \quad (16)$$

The anti-instanton contributions follow similarly. The PDF follows from the double limit of $z^2 \rightarrow 0$ and $P^z \rightarrow \infty$ but fixed zP^z . Hence, $z \approx 1/P^z \ll L$ justifying the use of the SIA with small size instantons. The gauge link can be reduced by noting that it Abelianizes along $\sigma_{z\nu} z_{I\nu}$,

$$[+\frac{z}{2}, -\frac{z}{2}]_I = \mathbf{P} e^{-i \int_{-\frac{z}{2}-z_{3I}}^{+\frac{z}{2}-z_{3I}} A_3^U(x_3 - \tilde{z}_I) dx_3} = \cos F(z, z_I) + i U^\dagger 2 \sigma_{z\nu} \hat{z}_{I\nu} U \sin F(z, z_I) \quad (17)$$

with $\bar{\eta}_{\mu\nu}^a T^a = \frac{1}{4i} (\bar{\sigma}_\mu \sigma_\nu - \bar{\sigma}_\nu \sigma_\mu) = \sigma_{\mu\nu}$, $\tilde{z}_I = (z_{\perp I}, 0, z_{4I}) \equiv (z_{1I}, z_{2I}, 0, z_{4I})$, and

$$\begin{aligned} F(z, z_I) = & \frac{1}{2} \left[\frac{\sqrt{z_{1I}^2}}{\sqrt{\tilde{z}_I^2}} \left(\tan^{-1} \left(\frac{z/2 - z_{3I}}{\sqrt{\tilde{z}_I^2}} \right) + \tan^{-1} \left(\frac{z/2 + z_{3I}}{\sqrt{\tilde{z}_I^2}} \right) \right) \right. \\ & \left. - \frac{\sqrt{z_{1I}^2}}{\sqrt{\tilde{z}_I^2 + \rho^2}} \left(\tan^{-1} \left(\frac{z/2 - z_{3I}}{\sqrt{\tilde{z}_I^2 + \rho^2}} \right) + \tan^{-1} \left(\frac{z/2 + z_{3I}}{\sqrt{\tilde{z}_I^2 + \rho^2}} \right) \right) \right] \end{aligned} \quad (18)$$

To project onto the left- or right-handed Dirac spinors in (16), it is sufficient to keep only the terms proportional to \mathcal{P}_\pm in the LSZ reduced quark propagators (10-12), with the result

$$\tilde{f}(z, P^z) = 2 \times e^{izP^z} \text{Tr}_c \left[\frac{2}{\sqrt{\Pi_+} \sqrt{\Pi_-}} \left(A_+ \tilde{A}_- \right) \right] \quad (19)$$

Note that the overall factor of 2 takes care of the anti-instanton contribution, with the definitions (before subtraction)

$$\begin{aligned}
A_+ &= \frac{1}{2} + \frac{\rho^2}{4z_+^2} U \bar{p} \bar{z}_+ U^\dagger I_+^1, \\
\tilde{A}_- &= \frac{1}{2} + \frac{\rho^2}{4z_-^2} U z_- p U^\dagger I_-^1
\end{aligned} \tag{20}$$

and ($z_\pm = \pm z/2 - z_I$)

$$\Pi_\pm = \frac{1}{1 + \frac{\rho^2}{(z_\pm - z_I)^2}} = \frac{1}{1 + \frac{\rho^2}{(\pm z/2 - z_I)^2}} \tag{21}$$

Using the results $\text{Tr}_c(\bar{p}\bar{z}) = \text{Tr}_c P^z (1 - \sigma^z)(i\sigma^z z) = -2izP^z$, $\text{Tr}_c(pz) = 2iP^z z$ and $p\bar{p} = p^2 = 0$, we can simplify (19)

$$\text{Tr}_c A_+ \tilde{A}_- = \frac{1}{2} - \frac{\rho^2}{2N_c z_+^2} (iP^z z_+) (I_+^1) + \frac{\rho^2}{2N_c z_-^2} (iP^z z_-) (I_-^1) \tag{22}$$

and obtain (after subtraction)

$$\begin{aligned}
\tilde{f}(z^2, zP^z) &= n_{I+\bar{I}} \int d^4 z_I \left[e^{-izP^z} \left(\frac{1}{\sqrt{\Pi_+}} \frac{1}{\sqrt{\Pi_-}} - 1 \right) \cos F(z, z_I) \right. \\
&\quad \left. - \frac{1}{2N_c} \left(\frac{\rho^2}{z_+^2} \frac{(iP^z z_+)}{\sqrt{\Pi_+ \Pi_-}} - \frac{\rho^2}{z_-^2} \frac{(iP^z z_-)}{\sqrt{\Pi_+ \Pi_-}} \right) \cos F(z, z_I) \int_0^1 dt t e^{-i(t+1)zP^z/2} \right]
\end{aligned} \tag{23}$$

The integration over the z_I -position diverges quadratically, following the slow decay of the 2-point function in a quark on mass-shell. As noted earlier, this divergence is cutoff by the mean distance L to the nearest neighbor instanton or anti-instanton in the SIA, a simple way to factor in the effects of the inter-instanton interactions. With this in mind and since $F \rightarrow 0$ as $z \rightarrow 0$, the result is

$$n_{I+\bar{I}} \int d^4 z_I \left(\frac{1}{\sqrt{\Pi_+}} \frac{1}{\sqrt{\Pi_-}} - 1 \right) \cos F(z, z_I) \approx -\frac{\pi\sqrt{\kappa}}{2} + \mathcal{O}(z^2) \tag{24}$$

where we used that $n_{I+\bar{I}} = 1/L^4$ for a diluteness parameter $\kappa = \pi^2 \rho^4 n_{I+\bar{I}}$. The transmutation of the expansion from $\kappa \rightarrow \sqrt{\kappa}$ reflects on the screening-like effect, and is analogous to the one noted in [19]. Similarly we have

$$\frac{n_{I+\bar{I}}}{N_c} \int d^4 z_I \frac{\rho^2}{z_\pm^2} \frac{P^z z_\pm}{\sqrt{\Pi_+ \Pi_-}} \cos F(z, z_I) \approx \pm \frac{zP^z}{2N_c} n_{I+\bar{I}} \int d^4 z_I \frac{\rho^2}{z_\pm^2} \frac{1}{\sqrt{\Pi_+ \Pi_-}} \approx \pm \frac{zP^z}{2N_c} \pi\sqrt{\kappa} + \mathcal{O}(z^2) \tag{25}$$

In terms of the integral transform

$$\tilde{f}(z^2, \lambda = zP^z) = \int_0^1 dx e^{-ix\lambda} \tilde{f}(z^2, x) \quad (26)$$

the final one-loop instanton result at tree level is

$$\tilde{f}(z^2, x) \approx \frac{\pi\sqrt{\kappa}}{2} \left(\theta(x - 1/2)\theta(1 - x) - \delta(1 - x) \right) + \mathcal{O}(z^2, 1/N_c, \kappa) \rightarrow f(x) \quad (27)$$

This has the correct support in $[0, 1]$, and identifies with the light-cone PDF $f(x)$ as $z^2 \rightarrow 0$. The additional contributions to (23) stemming from the remaining cross terms in (16) with a similar behavior, are listed in Appendix D both for the $z = 0$ and the leading $z \neq 0$ terms for completeness.

B. Mixing

There is an additional mixed zero-mode and non-zero-mode contribution following from the cross contribution from the $\mathcal{O}(m)$ and $\mathcal{O}(1/m)$ in (6), with the result to order $\mathcal{O}(m^0)$

$$\begin{aligned} & \frac{n_{I+\bar{I}}}{2} \int d^4 z_I \int dU e^{iP^z z} \left(\frac{4\pi^2 \rho^3}{\Pi_+^{\frac{3}{2}} \Pi_-^{\frac{1}{2}}} \right) \left[(\bar{\chi}_R(P) \epsilon U) (U^\dagger \epsilon \bar{S}_0(z_+)) \sigma^z \right. \\ & \quad \times (\cos F(z, z_I) + i U^\dagger 2\sigma_{z\nu} \hat{z}_{I\nu} U \sin F(z, z_I)) \left(\frac{2\pi^2}{|\vec{p}|} - \frac{\pi^2 \rho^2}{z_-^2} \mathcal{P}_- U z_- U^\dagger I_+^0 \right) \chi_R(P) \left. \right] \\ & + \frac{n_{I+\bar{I}}}{2} \int d^4 z_I \int dU e^{iP^z z} \left(\frac{4\pi^2 \rho^3}{\Pi_-^{\frac{3}{2}} \Pi_+^{\frac{1}{2}}} \right) \left[\bar{\chi}_L(P) \bar{\sigma}^z \left(\frac{2\pi^2}{|\vec{p}|} - \frac{\pi^2 \rho^2}{z_+^2} \mathcal{P}_- U \bar{z}_+ U^\dagger I_+^0 \right) \right. \\ & \quad \times (\cos F(z, z_I) + i U^\dagger 2\sigma_{z\nu} \hat{z}_{I\nu} U \sin F(z, z_I)) S_0(z_-) \epsilon U (U^\dagger \epsilon \chi_L(P)) \left. \right] \end{aligned} \quad (28)$$

$\Pi_\pm \rightarrow 1$ at large z_I , and the integrand is dominated by $S_0(z_I)$, which is seen to integrate to zero for $z = 0$. The apparent linear divergence vanishes. (28) is at most logarithmically divergent in z_I which is cutoff by the mean distance L to the nearest neighbor, hence of order $\kappa \text{Log}(1/\kappa)$ and subleading in the diluteness expansion.

C. Comment on Current conservation

Here we briefly comment on the conservation for the vector current $J^\mu = \bar{\psi} \gamma^\mu \psi$ and the normalization of the PDF. At tree level, there is no matching effect, and the quasi-PDF normalizes to 1,

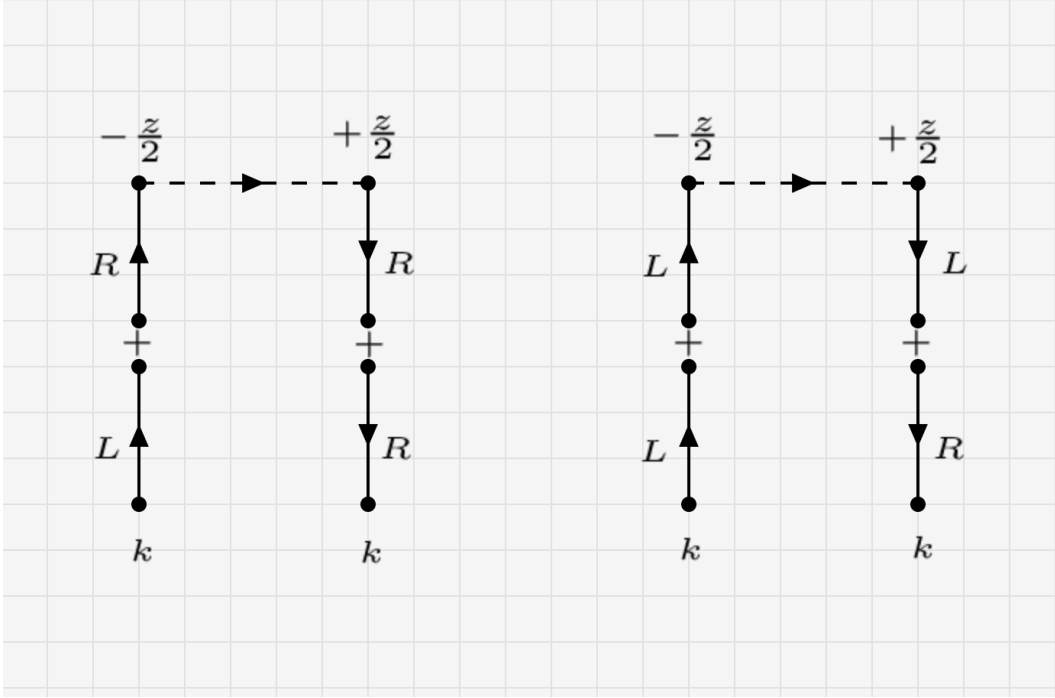


FIG. 2. Non-vanishing small instanton contributions to twist-2 matching factor from mixing between non-zero-modes and zero-modes.

$$\tilde{f}(z^2 = zP^z = 0) = 1 . \quad (29)$$

However, the density expansion to leading order in $\sqrt{\kappa}$ can differ from this canonical result. Additional charge renormalization is needed. Indeed, at $z = 0$, the quasi-PDF reads

$$\tilde{f}(0) = 1 + n_I \int d^4 z_I \tilde{f}^1(z_I) , \quad (30)$$

with

$$\tilde{f}^1(z_I) = \text{tr} \mathcal{P}_+ \sigma^z \mathcal{P}_+ \text{tr}_c \left(\frac{1}{4} \left(\frac{1}{\Pi_I} - 1 \right) - \frac{\rho^2}{8x_I^2} \frac{P^z}{N_c} (\mathcal{P}_- \bar{x}_I I_+^1 - x_I \mathcal{P}_+ I_-^1) \frac{1}{\Pi_I} \right) + \dots \quad (31)$$

where the dots stand for the $z = 0$ additional contributions listed in Appendix D. Clearly, these integrals are non-zero, and a charge renormalization $J^\mu \rightarrow ZJ^\mu$ is needed, with $Z = 1 + \sqrt{\kappa}Z_1(\kappa)$. This will enforce the condition $\tilde{f}(0) = 1$. At the quasi-PDF level, this means $\tilde{f} \rightarrow \tilde{f} + \delta(1-x)\sqrt{\kappa}Z_1(\kappa)$, which will normalize the quasi-PDF to 1.

D. Small instanton contributions: polarized distributions

The instanton contributions to the polarized quark PDF are illustrated in Fig. 2 with the result

$$\begin{aligned} & i \frac{n_{I+\bar{I}}}{2} \int d^4 z_I \bar{\chi}_L(P) i P \bar{S}(P, \frac{z}{2} - z_I) \sigma^z \bar{\sigma}^i [+\frac{z}{2}, -\frac{z}{2}]_I S(-\frac{z}{2} - z_I, P) i \bar{P} \chi_R(P) \\ & - i \frac{n_{I+\bar{I}}}{2} \int d^4 z_I \bar{\chi}_R(P) i \bar{P} S(P, \frac{z}{2} - z_I) \bar{\sigma}^z \sigma^i [+\frac{z}{2}, -\frac{z}{2}]_I \bar{S}(-\frac{z}{2} - z_I, P) i P \chi_L(P), \end{aligned} \quad (32)$$

The anti-instanton contribution follows similarly and will be added at the end. We apply the same rules to unwind the matrix elements in (32), with the result ($z_\pm = \pm z/2 - z_I$)

$$\begin{aligned} & i \frac{n_{I+\bar{I}}}{2} \int d^4 z_I \int dU e^{iPz} z \left(\frac{4\pi^2 \rho^3}{im\Pi_+^{\frac{3}{2}}} \right) \frac{1}{\sqrt{\Pi_-}} \\ & \times \left((\bar{\chi}_L(P) \epsilon U) (U^\dagger \epsilon \bar{S}_0(z_+)) \sigma^z \bar{\sigma}^i (\cos F(z, z_I) + i U^\dagger 2\sigma_{z\nu} \hat{z}_{I\nu} U \sin F(z, z_I)) \chi_R(P) \right) \\ & - i \frac{n_{I+\bar{I}}}{2} \int d^4 z_I \int dU e^{iPz} z \left(\frac{4\pi^2 \rho^3}{im\Pi_-^{\frac{3}{2}}} \right) \frac{1}{\sqrt{\Pi_+}} \\ & \times \left((\bar{\chi}_R(P) \bar{\sigma}^z \sigma^i (\cos F(z, z_I) + i U^\dagger 2\sigma_{z\nu} \hat{z}_{I\nu} U \sin F(z, z_I)) S_0(z_-) \epsilon U) (U^\dagger \epsilon \chi_L(P)) \right) \end{aligned} \quad (33)$$

with $S_0(z_-) = z_-/(2\pi^2 z_-^4)$ and $\bar{S}_0(z_+) = z_+/(2\pi^2 z_+^4)$. The reduction of the zero modes is given in Appendix B. The chirality flip is seen to follow from the mixing between the zero modes and the non-zero modes.

After carrying the averaging over the instanton moduli, only the cos-term contribution in (33) survives. The sin-term vanishes after the z_I -integration since $\sigma_{zz} = 0$. With this in mind and adding the contribution of the anti-instanton through $R \leftrightarrow L$ and conjugation through the bar-assignment for σ^μ , we obtain

$$\begin{aligned} & e^{iPz} z \frac{\kappa z}{\rho N_c} \left(\mathcal{J}_+(z) \bar{\chi}_L(P) \frac{\bar{\sigma}^z \sigma^z \bar{\sigma}^i}{2m} \chi_R(P) + \mathcal{J}_-(z) \bar{\chi}_R(P) \frac{\bar{\sigma}^z \sigma^i \sigma^z}{2m} \chi_L(P) \right) \\ & + e^{iPz} z \frac{\kappa z}{\rho N_c} \left(\mathcal{J}_+(z) \bar{\chi}_R(P) \frac{\sigma^z \bar{\sigma}^z \sigma^i}{2m} \chi_L(P) + \mathcal{J}_-(z) \bar{\chi}_L(P) \frac{\sigma^z \bar{\sigma}^i \bar{\sigma}^z}{2m} \chi_R(P) \right) \end{aligned} \quad (34)$$

with the diluteness factor $\kappa = \pi^2 \rho^4 n_{I+\bar{I}}$ and

$$\mathcal{J}_{\pm}(z) = \frac{1}{2\pi^2} \int \frac{d^4 z_I}{z_I^4} \left(\frac{1}{1 + \frac{\rho^2}{z_I^2}} \right)^{\frac{3}{2}} \left(\frac{1}{1 + \frac{\rho^2}{z_{\pm} z_I^2}} \right)^{\frac{1}{2}} \cos F(z, z_I \pm z/2) \approx \frac{1}{4} \text{Log} \left(\frac{1}{\kappa} \right) + \mathcal{O}(z^2) \quad (35)$$

The SIA contribution to the polarized quasi-PDF is of order $\kappa \text{Log}(1/\kappa)$, but vanishes as $z \rightarrow 0$ with no contribution to the polarized quark PDF.

V. INSTANTON CONTRIBUTION TO THE QUASI-PDF: GLUON-EXCHANGE AT ONE-LOOP LEVEL

In the previous section, we have investigated the ‘‘tree-level’’ contribution to the quasi-PDF in the instanton background. The matching effect turns out to be trivial. In this section we investigate a sample gluon-exchange diagram in the instanton background that has non-negligible matching effect.

A. Perturbative contribution in position space

To streamline the short distance contribution to the one-gluon exchange in the instanton background, we first consider its perturbative analogue

$$\begin{aligned} & e^{-iPz} \int d^4 x d^4 y e^{-iP \cdot (x-y)} g_s^2 C_F \Delta_0(x-y) \\ & \times \text{Tr} \left(\gamma_{\mu} S_0(x, \frac{z}{2}) \gamma^z [\frac{z}{2}, -\frac{z}{2}] S_0(-\frac{z}{2}, y) T^b \gamma_{\mu} \chi(P) \chi^{\dagger}(P) \right) \\ \rightarrow & e^{-iPz} \int d^4 x d^4 y e^{-iP \cdot (x-y)} \frac{g_s^2 C_F}{2(2\pi^2)^3} \frac{1}{(x-y)^2} \frac{1}{(x - \frac{z}{2})^4} \frac{1}{(y + \frac{z}{2})^4} \\ & \times \text{Tr} \left(\gamma_{\mu} \gamma \cdot (x - \frac{z}{2}) \gamma^z [\frac{z}{2}, -\frac{z}{2}] \gamma \cdot (-\frac{z}{2} - y) \gamma_{\mu} \not{P} \right) \end{aligned} \quad (36)$$

with $C_F = (N_c^2 - 1)/2$ and after setting the gauge link to 1 to probe the leading singularity. The integral in (36) can be performed in position space by shifting $x - z/2 \rightarrow x + \frac{r}{2}$ and $y + z/2 \rightarrow x - \frac{r}{2}$, with the result

$$\frac{\alpha_s C_F}{4\pi^4} \int d^4 x d^4 r \frac{\text{Tr} \gamma \cdot (x + \frac{r}{2}) \gamma^z \gamma \cdot (x - \frac{r}{2}) (\gamma^0 - \gamma^z)}{(x + \frac{r}{2})^4 (x - \frac{r}{2})^4 (r+z)^2} e^{-iPz - iP \cdot r} \quad (37)$$

The integral in x can be undone

$$\int d^4x \frac{\text{Tr} \gamma \cdot (x + \frac{r}{2}) \gamma^z \gamma \cdot (x - \frac{r}{2}) (\gamma^0 - \gamma^z)}{(x + \frac{r}{2})^4 (x - \frac{r}{2})^4} = -8\pi^2 \frac{r^0 r^z - (r^0)^2 + r_\perp^2}{r^4} \quad (38)$$

leading (37) in the form

$$-\frac{2\alpha_s C_F e^{-iPz}}{\pi^2} \int d^4r e^{-iP \cdot r} \frac{r^0 r^z - (r^0)^2 + r_\perp^2}{r^4 (r+z)^2}. \quad (39)$$

In Euclidean space, one has $x^0 = -ix^4$, thus one has to evaluate the integral

$$-\frac{2\alpha_s C_F e^{-iPz}}{\pi^2} \int d^4r e^{-iP \cdot r} \frac{-ir^4 r^z + (r^4)^2 + r_\perp^2}{r^4 (r+z)^2}. \quad (40)$$

and then analytic continue to the value $P^2 = 0$. By using a Feynman parametrization, one has

$$-\frac{4\alpha_s C_F e^{-iPz}}{\pi^2} \int_0^1 dt (1-t) e^{iPz t} \int d^4r e^{-iP \cdot r} \frac{-ir^4 r^z + (r^4)^2 + r_\perp^2}{(r^2 + t(1-t)z^2)^3}. \quad (41)$$

The last integral can be evaluated

$$\begin{aligned} & \int d^4r e^{-iP \cdot r} \frac{-ir^4 r^z + (r^4)^2 + r_\perp^2}{(r^2 + t(1-t)z^2)^3} \\ &= - \left(i \frac{\partial}{\partial P^4} \frac{\partial}{\partial P^z} + \frac{\partial^2}{\partial (P^4)^2} + \frac{\partial^2}{\partial P_\perp^2} \right) \int d^4r e^{-iP \cdot r} \frac{1}{(r^2 + t(1-t)z^2)^3}, \end{aligned} \quad (42)$$

which exhibits the desired singularity as $z^2 \rightarrow 0$.

Now we can use the relation between the quasi PDF \tilde{f} and the PDF f in position space to extract the matching kernel C .

$$\tilde{f}(z^2, \lambda = zP^z) = \int_0^1 d\alpha C(z^2, \alpha) f(\alpha\lambda) \quad (43)$$

The iteration of (43) to one-loop gives

$$\tilde{f}^{(1)}(z^2, \lambda) - f^{(1)}(\lambda) = \int_0^1 d\alpha C^{(1)}(z^2, \alpha) e^{i\alpha\lambda} \quad (44)$$

Factorisation follows if (44) admits an IR safe solution kernel $C^{(1)}$. Note that the loop-expansion can be sought either in perturbation theory, or semi-classically as we already discussed at tree level. We now proceed to the semi-classical one-loop correction.

B. Gluon exchange in the instanton background

The gluon propagator in the instanton background is obtained using the decomposition $A_\mu = A_{I\mu} + a_\mu$ in the YM action to quadratic order in the covariant background field gauge $D_\mu a_\mu = (\partial_\mu - iA_{I\mu})a_\mu = 0$,

$$\frac{1}{2}a_\mu \left(-D^2\delta_{\mu\nu} - 2[D_\mu, D_\nu] + \left(\frac{1}{\alpha} - 1\right)D_\mu D_\nu \right) a_\nu \quad (45)$$

The instanton with collective variables $\xi_i = \lambda_i, \rho, Z_i$ is characterized by

$$[(N_c^2 - 1) - (N_c - 2)^2] + 1 + 4 = 4N_c$$

zero modes $\phi_\mu^i = \partial A_\mu(x, \xi_i)/\partial \xi_i$. As a result, the gauge-fixed gluon propagator follows from the inversion

$$\left(-D^2\delta_{\mu\nu} - 2[D_\mu, D_\nu] + \left(\frac{1}{\alpha} - 1\right)D_\mu D_\nu \right) \Delta_{\mu\nu}(x, y) = \delta_{\mu\nu}\delta^4(x - y) - \sum_{i=1}^{4N_c} \phi_\mu^i(x)\phi_\nu^{i\dagger}(y) \quad (46)$$

The inversion can be obtained in closed form [22]

$$\Delta_{\mu\nu}(x, y) = g_{\mu\nu\rho\sigma} iD_\rho \Delta_2(x, y) iD_\sigma + (\alpha - 1) iD_\mu \Delta_2(x, y) iD_\nu \quad (47)$$

in terms of the squared scalar propagator in the instanton background

$$\Delta_2(x, y) = \int d^4z \Delta(x, z)\Delta(z, y) \quad (48)$$

with

$$\Delta^{ab}(x, y) = \Delta_0(x - y) \left(1 + \rho^2 \frac{[Ux\bar{y}U^\dagger]}{x^2 y^2} \right)^{ab} \frac{1}{\sqrt{\Pi_x \Pi_y}} \quad (49)$$

and with the free scalar propagator $\Delta_0(x) = 1/(2\pi x)^2$, and

$$g_{\mu\nu\rho\sigma} = \left(\delta_{\mu\nu}\delta_{\rho\sigma} + \delta_{\mu\rho}\delta_{\nu\sigma} - \delta_{\mu\sigma}\delta_{\nu\rho} + \epsilon_{\mu\nu\rho\sigma} \right) \quad (50)$$

C. Non-perturbative contribution in position space

For the unpolarized PDF, the one-loop contribution in the instanton background follows the tree level contributions in Fig. 1 with an additional gluon ring through the instanton, that could attach to the pair of in-out quarks, the gauge-link or the quark-gauge link. For an estimate, consider the ring attached to the in-out quarks,

$$\begin{aligned}
& \frac{n_{I+\bar{I}}}{2} \int d^4 z_I \int d^4 x d^4 y \Delta_{\mu\nu}^{ab}(x, y) \bar{\chi}_R(P) i\bar{P}S(P, z_I + x) g_s T^a \bar{\sigma}_\mu S(x, z_I + \frac{z}{2}) \\
& \times \bar{\sigma}^z[\frac{z}{2}, -\frac{z}{2}]_I S(z_I - \frac{z}{2}, y) g_s T^b \bar{\sigma}_\nu S(z_I + y, P) i\bar{P}\chi_R(P) \\
& + \frac{n_{I+\bar{I}}}{2} \int d^4 z_I \int d^4 x d^4 y \Delta_{\mu\nu}^{ab}(x, y) \bar{\chi}_L(P) iP\bar{S}(P, z_I + x) g_s T^a \sigma_\mu \bar{S}(x, z_I + \frac{z}{2}) \\
& \times \sigma^z[\frac{z}{2}, -\frac{z}{2}]_I \bar{S}(z_I - \frac{z}{2}, y) g_s T^b \sigma_\nu S(z_I + y, P) iP\chi_L(P)
\end{aligned} \tag{51}$$

The anti-instanton contribution follows similarly and will be added at the end.

If we set the gauge link to 1, the insertion of the gluon propagator (47) simplifies, if we note that the $(\alpha-1)$ gauge dependent insertion drops on mass-shell. Also, the substitution

$$\epsilon_{\mu\nu\rho\sigma} iD_\rho \Delta_2(x, y) iD_\sigma = \frac{1}{2} \left(F_{\mu\nu}(x) \Delta_2(x, y) + \Delta_2(x, y) F_{\mu\nu}(y) \right) \tag{52}$$

using the self-duality of the the gauge field, vanishes after color tracing since $F_{\mu\nu}^{aa}(x) = 0$. Also, the contribution from the tensor part $(\delta_{\mu\rho}\delta_{\nu\sigma} - \delta_{\mu\sigma}\delta_{\nu\rho})$ vanishes for the in-out quark on mass shell through an integration by parts. With this in mind, we now carry the remainder of the non-vanishing contributions using

$$iD_\rho \Delta_2(x, y) iD_\rho = \Delta(x, y) = \Delta_0(x - y) \left(\frac{1}{\sqrt{\Pi_x \Pi_y}} + \mathcal{O}\left(\frac{1}{N_c}\right) \right) \tag{53}$$

or more specifically

$$\Delta_{\mu\nu}^{ab}(x, y) \rightarrow \delta^{ab} \delta_{\mu\nu} \Delta_0(x - y) \left(\frac{1}{\sqrt{\Pi_x \Pi_y}} + \mathcal{O}\left(\frac{1}{N_c}\right) \right) \tag{54}$$

where the second contribution in (49) is suppressed by $1/N_c$ after color averaging. Similarly,

$$\begin{aligned}
i\bar{P}S(P, z_I + x) & \rightarrow e^{-iP \cdot (z_I + x)} \frac{1}{\sqrt{\Pi_x}} + \mathcal{O}\left(\frac{1}{N_c}\right) \\
S(P, z_I + y) i\bar{P} & \rightarrow e^{+iP \cdot (z_I + y)} \frac{1}{\sqrt{\Pi_y}} + \mathcal{O}\left(\frac{1}{N_c}\right)
\end{aligned} \tag{55}$$

for the LSZ reduced quark propagator. Throughout, we are using the short-hand notation

$$\Pi_x = \frac{1}{1 + \frac{\rho^2}{(x-z_I)^2}} \quad \text{and} \quad \Pi_y = \frac{1}{1 + \frac{\rho^2}{(y-z_I)^2}} \quad (56)$$

Inserting (54-55) into (51), keeping only the leading fermion propagators in the loop in coordinate space to track the singular contribution, we obtain

$$\begin{aligned} & n_{I+\bar{I}} \frac{g_s^2 C_F}{2(2\pi^2)^3} \int d^4 z_I e^{-iPz} \int d^4 x d^4 y e^{-iP \cdot (x-y)} \\ & \times \frac{1}{(x-y)^2} \frac{1}{(x - \frac{z}{2})^4} \frac{1}{(y + \frac{z}{2})^4} \text{Tr} \left(\gamma_\mu \gamma \cdot (x - \frac{z}{2}) \gamma^z \gamma \cdot (-\frac{z}{2} - y) \gamma_\mu \not{P} \right) \\ & \times \left(\frac{1}{\sqrt{\Pi_x}} \frac{1}{\sqrt{\Pi_y}} \frac{1}{\sqrt{\Pi_x \Pi_y}} - 1 \right) \left(\frac{1}{\sqrt{\Pi_{x-z/2}}} \frac{1}{\sqrt{\Pi_{y+z/2}}} \right) \end{aligned} \quad (57)$$

The free contribution for $n_{I+\bar{I}} \rightarrow 1$ and $\rho \rightarrow 0$ is subtracted, as it amounts to the one-loop perturbative contribution evaluated earlier. Using the same change of variables as in (37), shifting the z_I integration variable,

$$\begin{aligned} x - z_I &\rightarrow x + \frac{r}{2} + \frac{z}{2} - z_I \rightarrow +\frac{r}{2} + \frac{z}{2} - z_I \equiv +(R_z - z_I) \\ y - z_I &\rightarrow x - \frac{r}{2} - \frac{z}{2} - z_I \rightarrow -\frac{r}{2} - \frac{z}{2} - z_I \equiv -(R_z + z_I) \end{aligned} \quad (58)$$

with $R_z = (r+z)/2$, and

$$\begin{aligned} x - \frac{z}{2} - z_I &\rightarrow x + \frac{r}{2} - z_I \rightarrow +\frac{r}{2} - z_I \equiv +(R - z_I) \\ y + \frac{z}{2} - z_I &\rightarrow x - \frac{r}{2} - z_I \rightarrow -\frac{r}{2} - z_I \equiv -(R + z_I) \end{aligned} \quad (59)$$

with $R = r/2$, and carrying the x-integration as in (37-40) we obtain

$$- \frac{g_s^2 C_F n_{I+\bar{I}} \rho^4}{2\pi^3} e^{-iPz} \int d^4 r e^{-iP \cdot r} \frac{-i r^4 r^z + (r^4)^2 + r_\perp^2}{r^4 (r+z)^2} \mathbf{F}(R_z, R) \quad (60)$$

The dimensionless instanton induced form factor in coordinate space is

$$\mathbf{F}(R_z, R) = \int \frac{d^4 z_I}{\rho^4} \left(\frac{1}{\sqrt{\Pi_{+R_z}}} \frac{1}{\sqrt{\Pi_{-R_z}}} \frac{1}{\sqrt{\Pi_{+R_z} \Pi_{-R_z}}} - 1 \right) \frac{1}{\sqrt{\Pi_{+R}}} \frac{1}{\sqrt{\Pi_{-R}}} \quad (61)$$

After a Feynman parametrization similar to (41), we finally get

$$-\frac{2g_s^2 C_F \kappa}{\pi^5} \int_0^1 dt (1-t) e^{iP^z t z} \int d^4 r e^{-iP \cdot r} \frac{-ir^4 r^z + (r^4)^2 + r_\perp^2}{(r^2 + t(1-t)z^2)^3} \mathbf{F}(R_z, R) \quad (62)$$

with the diluteness factor $\kappa = \pi^2 \rho^4 n_{I+\bar{I}}$. For $r, z \rightarrow 0$, the integral in (62) diverges logarithmically as in the one-loop perturbative case (42) but with a non-perturbative pre-factor

$$2 \times \left(-\frac{2g_s^2 C_F \kappa}{\pi^5} \right) \left(-\frac{2\pi^3}{\sqrt{\kappa}} \right) \int_0^1 dt (1-t) e^{iP^z t z} \int d^4 r e^{-iP \cdot r} \frac{-ir^4 r^z + (r^4)^2 + r_\perp^2}{(r^2 + t(1-t)z^2)^3} \quad (63)$$

with the extra factor of 2 accounting for the anti-instanton contribution, after using ($|z_I| \leq L$)

$$\mathbf{F}(0, 0) = \int d^4 z \left(\frac{1}{(1 + 1/z^2)^2} - 1 \right) \frac{1}{(1 + 1/z^2)} \approx -\frac{2\pi^3}{\sqrt{\kappa}} \quad (64)$$

D. Matching kernel and trans-series

To one-loop, the contribution of the instanton to the matching kernel amounts to a shift in the perturbative pre-factor by

$$-\frac{\alpha_s C_F}{\pi^2} \rightarrow -\frac{\alpha_s C_F}{\pi^2} \left(1 - 32\pi\sqrt{\kappa} \right) \quad (65)$$

The matching kernel coefficient develops into a trans-series [25] since at weak coupling $\sqrt{\kappa} \sim e^{-\pi/\alpha_s}$. As we noted earlier, cooled lattice simulations of the QCD vacuum suggest $\kappa \approx 1/10$ (regime of chiral symmetry breaking with large size instantons [15]) and $\kappa \approx 1$ (regime of short distance physics with small size instantons [16]). For both estimates, the small size instanton contribution in (65) is sizable in comparison to the perturbative one. It should be included when matching the quasi-PDF to the PDF in current lattice simulations.

VI. CONCLUSIONS

Cooled lattice gauge configurations display strongly inhomogeneous instanton and anti-instanton configurations. The dilute QCD instanton vacuum capture the essentials of these configurations. The small size instantons and anti-instantons involve strong gauge fields that contribute non-perturbatively to short distance physics without modifying the

essentials of the UV behavior. Using the SIA, we have shown how the instantons contribute sizably to the quark PDF in leading order. More importantly, although the matching effects is trivial at tree-level, we have found that they are part of a trans-series expansion of the matching kernel, that is dominant at one-loop. They should be considered in the current lattice extraction of the PDF's from their quasi-PDF counterparts.

We should emphasise that only the one-gluon contribution diagram has been considered, which is sufficient for our purpose of estimating the size of the effect. More detailed calculation with all diagrams included shall be provided somewhere else together with a calculation of the non-perturbative renormalization factors.

Acknowledgements This work is supported by the Office of Science, U.S. Department of Energy under Contract No. DE-FG-88ER40388.

Appendix A: Conventions

Following [20, 21, 26], we use the short hand matrix-valued notation $x \equiv \sigma_\mu x^\mu$ and $\bar{x} \equiv \bar{\sigma}_\mu x^\nu$, with the covariantized Pauli matrices in Euclidean and Minkowski space defined as

$$\begin{array}{lll} \text{Euclidean :} & \sigma_\mu = (1, -i\vec{\sigma}) & \bar{\sigma}_\mu = (1, +i\vec{\sigma}) & \sigma_\mu \bar{\sigma}_\nu + \sigma_\nu \bar{\sigma}_\mu = 2\eta_{\mu\nu} \\ \text{Minkowski :} & \sigma_\mu = (1, -\vec{\sigma}) & \bar{\sigma}_\mu = (1, +\vec{\sigma}) & \sigma_\mu \bar{\sigma}_\nu + \sigma_\nu \bar{\sigma}_\mu = 2g_{\mu\nu} \end{array}$$

with metric $g^{\mu\nu} = (+, -, -, -)$, $\eta^{\mu\nu} = \delta^{\mu\nu}$, and satisfying the identities

$$\sigma^\mu \bar{\sigma}^\nu - \sigma^\nu \bar{\sigma}^\mu = 2i\bar{\eta}^{a\mu\nu} \tau^a \quad \bar{\sigma}^\mu \sigma^\nu - \bar{\sigma}^\nu \sigma^\mu = 2i\eta^{a\mu\nu} \tau^a \quad (\text{A1})$$

with the η -tHooft symbol. The spinor indices are $\alpha, \beta = 1, 2$, and the color indices are $i, j = 1, 2, \dots, N_c$.

Our conventions for the γ^5 matrix in Euclidean and Minkowski space are respectively

$$\gamma_E^5 = \begin{pmatrix} -1 & 0 \\ 0 & 1 \end{pmatrix} \quad \gamma_M^5 = \begin{pmatrix} 1 & 0 \\ 0 & -1 \end{pmatrix} \quad (\text{A2})$$

In Weyl notations, the Euclidean Dirac spinor reads

$$\Psi(x) = \begin{pmatrix} K_\alpha^i(x) \\ \phi_i^\alpha(x) \end{pmatrix} \quad \Psi^\dagger(x) = (K_i^{\dagger\alpha}(x), \phi_\alpha^{\dagger i}(x)) \equiv (\bar{\phi}_i^\alpha(x), \bar{K}_\alpha^i(x)) \quad (\text{A3})$$

The Euclidean fermionic action splits into left K and right ϕ copies

$$\bar{K}\sigma \cdot (\partial - igA)K + \bar{\phi}\bar{\sigma} \cdot (\partial - igA)\phi \quad (\text{A4})$$

with $\bar{K} = \phi^\dagger$ and $\bar{\phi} = K^\dagger$ using

$$\gamma_E^\mu = \begin{pmatrix} 0 & \bar{\sigma}_E^\mu \\ \sigma_E^\mu & 0 \end{pmatrix} \quad \gamma_M^\mu = \begin{pmatrix} 0 & \bar{\sigma}_M^\mu \\ \sigma_M^\mu & 0 \end{pmatrix} \quad (\text{A5})$$

Appendix B: Fermionic zero modes

The instanton admits a left-handed zero mode $K_\alpha^i(x)$ satisfying $\sigma \cdot D K = 0$, and the anti-instanton a right-handed zero mode $\phi_i^\alpha(x)$ satisfying $\bar{\sigma} \cdot D \phi = 0$, which are eigenstates of $(1 \pm \gamma_E^5)/2$, and conjugate of each other. In terms of the Euclidean Weyl spinors, the instanton zero mode and its conjugate are

$$\begin{aligned} K_\alpha^i(x) &= \frac{\rho^{\frac{3}{2}}}{\pi x^4} \frac{(\bar{x}\epsilon U)_\alpha^i}{\Pi_x^{\frac{3}{2}}} = \frac{2\pi\rho^{\frac{3}{2}}}{\Pi_x^{\frac{3}{2}}} (\bar{S}_0(x)\epsilon U)_\alpha^i \\ K_i^{\dagger\alpha}(x) &= \frac{\rho^{\frac{3}{2}}}{\pi x^4} \frac{(U^\dagger\epsilon x)_i^\alpha}{x^4\Pi_x^{\frac{3}{2}}} = \frac{2\pi\rho^{\frac{3}{2}}}{\Pi_x^{\frac{3}{2}}} (U^\dagger\epsilon S_0(x))_i^\alpha \equiv \bar{\phi}_i^\alpha(x) \end{aligned} \quad (\text{B1})$$

Here ϵ is the antisymmetric spin 2-tensor with the normalization $\epsilon_{\alpha\sigma}\epsilon^{\sigma\beta} = \delta_\alpha^\beta$, and

$$\Pi_x = 1 + \frac{\rho^2}{x^2} \quad S_0(x) = \frac{x}{2\pi^2 x^4} \quad \bar{S}_0(x) = \frac{\bar{x}}{2\pi^2 x^4} \quad (\text{B2})$$

with $S_0(x)$ the free massless quark propagator. The zero modes are normalized to ρ ,

$$\int d^4x K^\dagger(x)K(x) = \rho \quad \int d^4x \phi^\dagger(x)\phi(x) = \rho \quad (\text{B3})$$

For the free Dirac spinors we will use the notation $\chi(k) = \chi_R(k) + \chi_L(k)$ (with Minkowski labeling) as the sum of free Weyl spinors, that satisfy

$$\not{k}\chi(k) = \not{k} \begin{pmatrix} \chi_R(k) \\ \chi_L(k) \end{pmatrix} = \begin{pmatrix} 0 & \bar{k} \\ k & 0 \end{pmatrix} \begin{pmatrix} \chi_R(k) \\ \chi_L(k) \end{pmatrix} = \begin{pmatrix} \bar{k}\chi_L(k) \\ k\chi_R(k) \end{pmatrix} = 0 \quad (\text{B4})$$

with the free-wave ortho-normalizations

$$\chi_{L,R}(k)\chi_{L,R}^\dagger(k) = k, \bar{k} \quad \chi_{L,R}^\dagger(k)\chi_{R,L}(k) = 0 \quad (\text{B5})$$

Appendix C: Details of the large time limit

In this Appendix we show how the large time limit in (9) can be taken. One can see that (9) consists of several contributions as in (5), with the last and more involved contribution

$$\int d^3\vec{y} e^{-i\vec{p}\cdot\vec{y}} \frac{(x\vec{y} - y^2)}{(x-y)^2 y^2} = \int d^3\vec{y} e^{-i\vec{p}\cdot\vec{y}} \frac{(x\vec{y})}{(x-y)^2 y^2} - \int d^3\vec{y} e^{-i\vec{p}\cdot\vec{y}} \frac{1}{(x-y)^2}, \quad (\text{C1})$$

with $y = (-T, \vec{y})$ and $x = (T_1, \vec{x})$. Note that $1/\Pi_y^{\frac{1}{2}}$ asymptotes 1 at large T . The second contribution in (C1) is the free scalar propagator and is readily integrated as detailed in the summary integrals below. The first contribution can be integrated through a Feynman parametrization followed by a change of variable $\vec{y} = t\vec{x} + \vec{z}$, to give

$$\begin{aligned} & x \int_0^1 dt \int d^3\vec{z} e^{-i\vec{p}\cdot\vec{z} - it\vec{p}\cdot\vec{x}} \frac{-T + it\vec{\sigma}\cdot\vec{x} + i\vec{\sigma}\cdot\vec{z}}{(\vec{z}^2 + (T+tT_1)^2 + (t-t^2)\vec{x}^2)^2} \\ &= \pi^2 x \int_0^1 dt (-T + it\vec{\sigma}\cdot\vec{x} - \sigma\cdot\vec{\nabla}_{\vec{p}}) \frac{e^{-|\vec{p}|\sqrt{(T+tT_1)^2 + (t-t^2)\vec{x}^2}}}{\sqrt{(T+tT_1)^2 + (t-t^2)\vec{x}^2}} \\ &\rightarrow e^{-|T||\vec{p}|} \left(\frac{-|\vec{p}| + \vec{\sigma}\cdot\vec{p}}{|\vec{p}|} \pi^2 x \int_0^1 dt e^{-t|\vec{p}|T_1 - it\vec{p}\cdot\vec{x}} + \mathcal{O}\left(\frac{1}{|T|}\right) \right). \end{aligned} \quad (\text{C2})$$

Similarly, consider the left reduction of \bar{S}

$$\lim_{T \rightarrow \infty} \int d^3\vec{x} \bar{S}(T, \vec{x}; y) e^{i\vec{p}\cdot\vec{x}} \quad (\text{C3})$$

which consists also of several contributions in (5). The last and involved contribution

$$\int d^3\vec{y} e^{i\vec{p}\cdot\vec{y}} \frac{y\bar{\sigma}^\mu(y-x)}{(y^2)^2(y-x)^2}, \quad (\text{C4})$$

can be unwound and evaluated through a Feynman parametrization

$$\begin{aligned} & 2 \int (1-t) dt \int d^3\vec{z} e^{i\vec{p}\cdot\vec{z} + it\vec{p}\cdot\vec{x}} \frac{(T - i\vec{\sigma}\cdot\vec{z} - it\vec{\sigma}\cdot\vec{x})\bar{\sigma}^\mu(T - T_1 - i\vec{\sigma}\cdot\vec{z} + i(1-t)\vec{\sigma}\cdot\vec{x})}{(\vec{z}^2 + (T-tT_1)^2 + (t-t^2)\vec{x}^2)^3} \\ &\rightarrow e^{-|T||\vec{p}|} \frac{\pi^2 |\vec{p}|}{2} \left(1 + \frac{\vec{\sigma}\cdot\vec{p}}{|\vec{p}|}\right) \bar{\sigma}^\mu \left(1 + \frac{\vec{\sigma}\cdot\vec{p}}{|\vec{p}|}\right) \int_0^1 dt (1-t) e^{T_1 t |\vec{p}| + it\vec{p}\cdot\vec{x}} \end{aligned} \quad (\text{C5})$$

at large T . Finally, we consider last

$$\int d^3\vec{y} e^{i\vec{p}\cdot\vec{y}} \frac{(\vec{y} - \vec{x})Uy\vec{x}U^\dagger}{(y-x)^4 y^2} . \quad (\text{C6})$$

A rerun of the preceding arguments give

$$e^{-|T||\vec{p}|} \frac{\pi^2 |\vec{p}|}{2} \left(1 - \frac{\vec{\sigma} \cdot \vec{p}}{|\vec{p}|}\right) U \left(1 + \frac{\vec{\sigma} \cdot \vec{p}}{|\vec{p}|}\right) \vec{x} U^\dagger \int_0^1 dt t e^{T_1 t |\vec{p}| + i t \vec{p} \cdot \vec{x}} \quad (\text{C7})$$

at large T .

We now note that the free propagators at large T read

$$\int d^3\vec{y} e^{i\vec{p}\cdot\vec{y}} \frac{\vec{y} - \vec{x}}{2\pi^2 (y-x)^4} \rightarrow \frac{e^{-|T||\vec{p}|}}{2} \left(1 - \frac{\vec{\sigma} \cdot \vec{p}}{|\vec{p}|}\right) e^{T_1 |\vec{p}| + i\vec{p}\cdot\vec{x}} \quad (\text{C8})$$

$$\int d^3\vec{y} e^{-i\vec{p}\cdot\vec{y}} \frac{\vec{x} - \vec{y}}{2\pi^2 (y-x)^4} \rightarrow \frac{e^{-|T||\vec{p}|}}{2} \left(1 - \frac{\vec{\sigma} \cdot \vec{p}}{|\vec{p}|}\right) e^{-T_1 |\vec{p}| - i\vec{p}\cdot\vec{x}} \quad (\text{C9})$$

$$\int d^3\vec{y} e^{-i\vec{p}\cdot\vec{y}} \frac{1}{(x-y)^2} \rightarrow \frac{2\pi^2}{|\vec{p}|} e^{-T_1 |\vec{p}| - i\vec{p}\cdot\vec{x}} \quad (\text{C10})$$

qpdf1 unpolarized

Appendix D: All terms for the quasi-PDF

Here, we list all the contributions to the quasi-PDF discussed in section IV A for completeness. All the contributions to the quasi-PDF at $z = 0$ are

$$A = \text{tr} \mathcal{P}_+ \sigma^z \mathcal{P}_+ \text{tr}_c \left(\frac{1}{4} \left(\frac{1}{\sqrt{\Pi_I}} - 1 \right)^2 - \frac{\rho^2}{8x_I^2 N_c} P^z (\mathcal{P}_- \bar{x}_I I_+^1 - x_I \mathcal{P}_+ I_-^1) \frac{1}{\Pi_I} \right) \quad (\text{D1})$$

$$B = -\text{tr} \mathcal{P}_+ \sigma^z \bar{\sigma}_\mu \text{tr}_c x_I \bar{\sigma}_\mu x_I \mathcal{P}_+ I_- \frac{\rho^2}{8N_c x_I^4 \Pi_I^2} \quad (\text{D2})$$

$$C = \text{tr} \mathcal{P}_+ \sigma^z \bar{\sigma}_\mu \text{tr}_c x_I \bar{\sigma}_\mu \frac{\rho^2}{4N_c x_I^4 p^z \Pi_I^2} \quad (\text{D3})$$

$$D = \text{tr} \mathcal{P}_+ \sigma^z \bar{\sigma}_\mu \text{tr}_c \mathcal{P}_- \bar{x}_I x_I \sigma^\mu \frac{\rho^4}{8N_c x_I^6 \Pi_I^2} I_+^1 \quad (\text{D4})$$

$$E = -\text{tr} \bar{\sigma}^\mu \sigma^z \mathcal{P}_+ \text{tr}_c \mathcal{P}_- \sigma_\mu \mathcal{P}_- \bar{x}_I p^z \frac{\rho^2}{8N_c x_I^2 \Pi_x} I_+ \quad (\text{D5})$$

$$F = -\text{tr} \bar{\sigma}^\mu \sigma^z \bar{\sigma}_{\mu'} \text{tr}_c \mathcal{P}_- \sigma_\mu \mathcal{P}_- \bar{x}_I x_I \sigma^{\mu'} \frac{\rho^4}{16N_c x_I^6 \Pi_I^2} I_+ . \quad (\text{D6})$$

Similarly, the full five contributions to the quasi-PDF at $z \neq 0$ are

$$B = -\text{tr}\mathcal{P}_+\sigma^z\bar{\sigma}_\mu\text{tr}_c x_I^+\bar{\sigma}_\mu x_I^-\mathcal{P}_+I_- \frac{\rho^2}{8N_c(x_I^-)^4\sqrt{\Pi_I^+(\Pi_I^-)^{\frac{3}{2}}}} \quad (\text{D7})$$

$$C = \text{tr}\mathcal{P}_+\sigma^z\bar{\sigma}_\mu\text{tr}_c x_I^-\bar{\sigma}_\mu \frac{\rho^2}{4N_c(x_I^-)^4\sqrt{\Pi_I^+(\Pi_I^-)^{\frac{3}{2}}}} \quad (\text{D8})$$

$$D = \text{tr}\mathcal{P}_+\sigma^z\bar{\sigma}_\mu\text{tr}_c\mathcal{P}_-\bar{x}_I^+x_I^-\sigma^\mu \frac{\rho^4}{8N_c(x_I^+)^2(x_I^-)^4\sqrt{\Pi_I^+(\Pi_I^-)^{\frac{3}{2}}}}I_+^1 \quad (\text{D9})$$

$$E = -\text{tr}\bar{\sigma}^\mu\sigma^z\mathcal{P}_+\text{tr}_c\mathcal{P}_-\sigma_\mu\mathcal{P}_-\bar{x}_I^+p^z \frac{\rho^2}{8N_c(x_I^+)^2\sqrt{\Pi_I^+\Pi_I^-}}I_+ \quad (\text{D10})$$

$$F = -\text{tr}\bar{\sigma}^\mu\sigma^z\bar{\sigma}_{\mu'}\text{tr}_c\mathcal{P}_-\sigma_\mu\mathcal{P}_-\bar{x}_I^+x_I^-\sigma^{\mu'} \frac{\rho^4}{16N_c(x_I^+)^2(x_I^-)^4\sqrt{\Pi_I^+(\Pi_I^-)^{\frac{3}{2}}}}I_+ . \quad (\text{D11})$$

In section IV A and for the purpose of estimating the speed of convergence of the quasi-PDF to the PDF in the large P^z limit, we have only considered the contribution corresponding to the terms in A .

-
- [1] X. Ji, *Phys. Rev. Lett.* **110**, 262002 (2013), [arXiv:1305.1539 \[hep-ph\]](#).
 - [2] J.-H. Zhang, J.-W. Chen, X. Ji, L. Jin, and H.-W. Lin, *Phys. Rev. D* **95**, 094514 (2017), [arXiv:1702.00008 \[hep-lat\]](#).
 - [3] X. Ji, A. Schäfer, X. Xiong, and J.-H. Zhang, *Phys. Rev. D* **92**, 014039 (2015), [arXiv:1506.00248 \[hep-ph\]](#).
 - [4] G. S. Bali, V. M. Braun, B. Gläsel, M. Göckeler, M. Gruber, F. Hutzler, P. Korcyl, A. Schäfer, P. Wein, and J.-H. Zhang, *Phys. Rev. D* **98**, 094507 (2018), [arXiv:1807.06671 \[hep-lat\]](#).
 - [5] C. Alexandrou, K. Cichy, M. Constantinou, K. Jansen, A. Scapellato, and F. Steffens, *Phys. Rev. D* **98**, 091503 (2018), [arXiv:1807.00232 \[hep-lat\]](#).
 - [6] T. Izubuchi, L. Jin, C. Kallidonis, N. Karthik, S. Mukherjee, P. Petreczky, C. Shugert, and S. Syritsyn, *Phys. Rev. D* **100**, 034516 (2019), [arXiv:1905.06349 \[hep-lat\]](#).
 - [7] T. Izubuchi, X. Ji, L. Jin, I. W. Stewart, and Y. Zhao, *Phys. Rev. D* **98**, 056004 (2018), [arXiv:1801.03917 \[hep-ph\]](#).
 - [8] X. Ji, Y. Liu, and I. Zahed, *Phys. Rev. D* **99**, 054008 (2019), [arXiv:1807.07528 \[hep-ph\]](#).
 - [9] A. V. Radyushkin, *Phys. Rev. D* **95**, 056020 (2017), [arXiv:1701.02688 \[hep-ph\]](#).
 - [10] Y.-Q. Ma and J.-W. Qiu, *Phys. Rev. D* **98**, 074021 (2018), [arXiv:1404.6860 \[hep-ph\]](#).

- [11] M. C. Chu, J. M. Grandy, S. Huang, and J. W. Negele, *Phys. Rev. D* **49**, 6039 (1994), [arXiv:hep-lat/9312071](#).
- [12] X. Ji, Y.-S. Liu, Y. Liu, J.-H. Zhang, and Y. Zhao, (2020), [arXiv:2004.03543 \[hep-ph\]](#).
- [13] E. Shuryak and I. Zahed, (2020), [arXiv:2008.06169 \[hep-ph\]](#).
- [14] E. V. Shuryak, *Nucl. Phys. B* **203**, 93 (1982).
- [15] T. Schäfer and E. V. Shuryak, *Rev. Mod. Phys.* **70**, 323 (1998), [arXiv:hep-ph/9610451](#).
- [16] A. Athenodorou, P. Boucaud, F. De Soto, J. Rodríguez-Quintero, and S. Zafeiropoulos, *JHEP* **02**, 140 (2018), [arXiv:1801.10155 \[hep-lat\]](#).
- [17] A. Hasenfratz, *Phys. Lett. B* **476**, 188 (2000), [arXiv:hep-lat/9912053](#).
- [18] E. V. Shuryak, (1999), [arXiv:hep-ph/9909458](#).
- [19] A. Kock, Y. Liu, and I. Zahed, *Phys. Rev. D* **102**, 014039 (2020), [arXiv:2004.01595 \[hep-ph\]](#).
- [20] I. I. Balitsky, M. Beneke, and V. M. Braun, *Phys. Lett. B* **318**, 371 (1993), [arXiv:hep-ph/9309217](#).
- [21] S. Moch, A. Ringwald, and F. Schrempp, *Nucl. Phys. B* **507**, 134 (1997), [arXiv:hep-ph/9609445](#).
- [22] L. S. Brown, R. D. Carlitz, D. B. Creamer, and C.-k. Lee, *Phys. Rev. D* **17**, 1583 (1978).
- [23] N. Andrei and D. J. Gross, *Phys. Rev. D* **18**, 468 (1978).
- [24] P. Faccioli and E. V. Shuryak, *Phys. Rev. D* **64**, 114020 (2001), [arXiv:hep-ph/0106019](#).
- [25] G. V. Dunne and M. Ünsal, *Phys. Rev. D* **89**, 041701 (2014), [arXiv:1306.4405 \[hep-th\]](#).
- [26] S. Vandoren and P. van Nieuwenhuizen, (2008), [arXiv:0802.1862 \[hep-th\]](#).